Enhancement of struvite pellets crystallization in a full-scale plant using an industrial grade magnesium product

D. Crutchik, N. Morales, J. R. Vázquez-Padín and J. M. Garrido

ABSTRACT

A full-scale struvite crystallization system was operated for the treatment of the centrate obtained from the sludge anaerobic digester in a municipal wastewater treatment plant. Additionally, the feasibility of an industrial grade $Mg(OH)_2$ as a cheap magnesium and alkali source was also investigated. The struvite crystallization plant was operated for two different periods: period I, in which an influent with low phosphate concentration (34.0 mg $P{\cdot}L^{-1}$) was fed to the crystallization plant; and period II, in which an influent with higher phosphate concentration (68.0 mg $P{\cdot}L^{-1}$) was used. A high efficiency of phosphorus recovery by struvite crystallization was obtained, even when the effluent treated had a high level of alkalinity. Phosphorus recovery percentage was around 77%, with a phosphate concentration in the effluent between 10.0 and 30.0 mg $P{\cdot}L^{-1}$. The experiments gained struvite pellets of 0.5–5.0 mm size. Moreover, the consumption of $Mg(OH)_2$ was estimated at 1.5 mol Mg added·mol P recovered^{-1}. Thus, industrial grade $Mg(OH)_2$ can be an economical alternative as magnesium and alkali sources for struvite crystallization at industrial scale.

Key words | industrial magnesium hydroxide, municipal wastewater, phosphorus recovery, struvite pellets

D. Crutchik (corresponding author)
J. M. Garrido
Department of Chemical Engineering, Institute of Technology,
University of Santiago de Compostela,
Santiago de Compostela 15782,
Spain
E-mail: *dafne.crutchik@gmail.com*

D. Crutchik
Faculty of Engineering and Sciences,
Universidad Adolfo Ibáñez,
Diagonal Las Torres 2640,
Santiago,
Chile

N. Morales
J. R. Vázquez-Padín
FCC Aqualia, Guillarei WWTP,
Camino de la Veiga s/n,
Tui E-36720,
Spain

INTRODUCTION

The crystallization of struvite ($MgNH_4PO_4{\cdot}6H_2O$) could be a sustainable and economical alternative for recovering phosphorus from wastewater. The principles of struvite formation, as well as the optimum operating conditions for struvite crystallization at bench scale, have been extensively studied (Rahman *et al.* 2014). However, only few struvite crystallization studies have been conducted at full scale. Some of these technologies developed at full scale are Unitika Phosnix© process, Ostara PEARL© process, Phospaq™ process and NuReSys© process. The Unitika Phosnix process is based on the struvite crystallization in a fluidized bed reactor (FBR), in which the crystallization of struvite is promoted by adding NaOH and $Mg(OH)_2$ as alkali and magnesium sources, respectively. The Ostara PEARL is a process, based on using a two-phase FBR. This system is composed of a column comprising a number of sections. The diameter of the column increases stepwise between the sections. This technology uses MgCl, when required, and NaOH to facilitate the struvite crystallization (Koch *et al.* 2009). The Phospaq process recovers phosphorus in a continuously aerated and agitated reactor. In this technology struvite crystallization is facilitated by the increase of pH via stripping of carbon dioxide (CO_2) and the addition of MgO as magnesium source (Remy *et al.* 2013). The NuReSys process is based on two completely stirred tanks: a stripping reactor and a stirred crystallization reactor, in which MgCl and NaOH are added to promote struvite crystallization (Moerman *et al.* 2009).

Struvite crystallization is recommended for wastewater streams with high phosphate concentration. Dockhorn (2009) performed an economic analysis and stated that the operating costs of struvite are reliant on phosphate concentration, in a way that the costs decrease with increasing phosphate concentration. So, phosphate concentrations should be above 50 mg PO_4^{3-}-$P{\cdot}L^{-1}$ in order to guarantee the economic viability of the process (Dockhorn 2009; Desmidt *et al.* 2013). Other authors reported a minimum phosphate concentration of 60 mg PO_4^{3-}-$P{\cdot}L^{-1}$ (Rahman *et al.* 2014). These values have been observed in different types of wastewater, such as swine wastewater, agro-industrial effluents, anaerobic liquor from primary and secondary sludge digestion, urine, and wastewater from

doi: 10.2166/wst.2016.527

food processing factories (Rahman *et al.* 2014). Generally, wastewater contains less magnesium compared with phosphate and ammonium, and the addition of a magnesium source to promote struvite crystallization is often required. The use of high grade magnesium sources, such as $MgCl_2$, $MgSO_4$, MgO or $Mg(OH)_2$, has been reported in other studies (Rahman *et al.* 2014). Nevertheless, the use of these high grade products can lead to high operating costs, compromising the viability of the process. The use of low cost magnesium sources, such as industrial grade MgO or $Mg(OH)_2$, can significantly reduce the operating costs.

One of the main challenges of struvite crystallization is the formation of undesirable small crystals. These fine crystals are often washed out with treated effluent, affecting the quality of the treated effluent as well as the economical viability of the crystallization process. Moreover, fine crystals diminish the market value of struvite as fertilizer (Forrest *et al.* 2008). For this reason, it is important to promote the growth of fine crystals, obtaining struvite pellets with a suitable size (>1.0 mm) to market the produced struvite efficiently. In this regard, the chosen crystallization system must be able to recover the phosphorus from wastewater in an efficient and economical way, converting it into granular product, struvite pellets, which could be commercialized as agricultural fertilizer.

The main aim of this study was to design and operate an innovative full-scale struvite crystallization plant. The crystallization plant was developed to (i) recover phosphorus in the form of struvite pellets and (ii) determine the viability of a low cost industrial grade $Mg(OH)_2$ slurry as magnesium and alkali sources for struvite crystallization.

MATERIALS AND METHODS

Experimental set-up and operating strategy

Crystallization system description

This study was carried out by operating a struvite crystallization plant at full scale, which was located in the municipal wastewater treatment plant (WWTP) of Guillarei (Galicia, NW Spain). The crystallization plant was composed of a 125 L two-phase FBR connected in series to a 3,260 L settler, and a $Mg(OH)_2$ slurry unit (Figure 1).

The FBR had a two-phase solid–liquid separator designed for separating the treated wastewater from

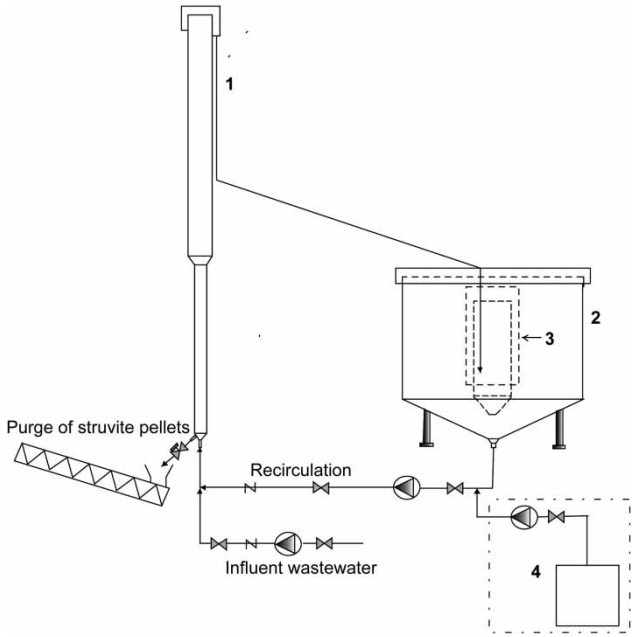

Figure 1 | Diagram of the struvite crystallization plant: (1) two-phase FBR; (2) settler; (3) central distribution system; (4) industrial $Mg(OH)_2$ slurry unit.

struvite pellets. The FBR was composed of two different cross-sectional areas, the top section and the bottom section, designed for maintaining the larger crystals (pellets) fluidized inside the FBR and promoting their growth (Figure 1). A weir was located at the top of the FBR in order to provide a uniform outflow of the treated effluent and the fine precipitates. A purge valve was located at the bottom of the FBR and was used for struvite pellets harvesting.

The settler was designed to promote the growth and recovery of fine crystals of struvite (Figure 1). The settler had a central distribution system, which was composed of two concentric cylinders designed for achieving a uniform distribution of the treated effluent and fine precipitates from the FBR. The bottom of the settler was conical in order to collect a mixture of unreacted $Mg(OH)_2$ slurry and struvite fines, which were recycled back to the FBR. This allowed us to obtain a better use of the industrial $Mg(OH)_2$.

The $Mg(OH)_2$ slurry unit was composed of a hydration reactor (an adapted concrete mixer) and a tank to store the $Mg(OH)_2$ slurry. $Mg(OH)_2$ was prepared by hydrating industrial grade MgO at 75 °C with water and steam. Additionally, a dosing pump was used to inject the $Mg(OH)_2$ slurry through a point located in the recirculation of the settler.

The managing and the monitoring of the crystallization system were carried out using a supervisory control and data

acquisition (SCADA) sytem, which was connected to a programmable logic controller. The SCADA system was used to monitor the crystallization system operation focusing on the pH, conductivity, the level of influent tank, and the flows control. The SCADA system also allowed control of the equipment of the crystallization system and provided the information of operating parameters and the equipment operation. This information can be extracted directly from the database.

Operating strategy and influent

The centrate obtained after centrifuging the effluent of the anaerobic sludge digester was fed to the crystallization plant. The centrate was accumulated in a homogenization tank in order to homogenize inlet peak flows before the struvite crystallization plant. The crystallization plant was operated continuously. It is important to note that struvite crystallization was the only P recovery/removal process applied in this municipal WWTP located in a non-sensitive area.

The hydraulic retention time (HRT) was between 1.3 and 2.6 min for the FBR and 74.2–135.0 min for the settler. The HRT for the entire system was in the range of 75.5–137.6 min. The operating temperature of the crystallization plant was around 25 °C. An on/off control strategy was used to maintain the operating pH between 8.1 and 8.6 by adding industrial $Mg(OH)_2$ slurry. The study lasted for 52 days and was divided into two different experimental periods. Table 1 summarizes the composition of the centrate fed wastewater used during the experimental period.

Period I lasted from day 0 until day 24. At the first experimental day, struvite seed crystals were added to the FBR to promote the heterogeneous crystallization of struvite. A centrate fed wastewater with high alkalinity and ammonium concentrations was fed. Phosphate concentration was 1.1 ± 0.2 mmol $PO_4^{3-}\cdot L^{-1}$ (34 ± 6 mg-P·L^{-1}). Ammonium concentration (70.4 ± 3.1 mmol $NH_4^+\cdot L^{-1}$) in wastewater was higher than stoichiometric requirements; the molar ratio of PO_4^{3-}:NH_4^+ was 1.0:64.0. The bicarbonate concentration was similar to that of ammonia. Magnesium and calcium ions were also present in the influent, with Mg^{2+}:PO_4^{3-}:Ca^{2+} molar ratio of 0.5:1.0:1.5 (Table 1).

Table 1 | Characteristics of the centrate fed wastewater for the experimental operation

Parameter	Period I	Period II
pH	8.2 ± 0.2	8.1 ± 0.1
Conductivity (mS·cm^{-1})	7.7 ± 0.4	7.6 ± 0.2
PO_4^{3-} (mmol·L^{-1})	1.1 ± 0.2	2.2 ± 0.9
NH_4^+ (mmol·L^{-1})	70.4 ± 3.1	70.0 ± 6.8
Mg^{+2} (mmol·L^{-1})	0.5 ± 0.1	0.6 ± 0.1
Ca^{+2} (mmol·L^{-1})	1.6 ± 0.3	1.8 ± 0.2
HCO_3^- (mmol·L^{-1})	67.0 ± 2.7	63.6 ± 2.5
K^+ (mmol·L^{-1})	2.0 ± 0.2	2.3 ± 0.2

Period II was from day 25 until day 52. Influent composition was similar to period I; however, phosphate concentration was higher than for the previous period. Phosphate concentration increased to 2.2 ± 0.9 mmol $PO_4^{3-}\cdot L^{-1}$ (68 ± 28 mg-P·L^{-1}). The molar ratios of Mg^{2+}:PO_4^{3-}:NH_4^+ and Ca^{2+}:PO_4^{3-}:HCO_3^- were 0.3:1.0:32.0 and 0.8:1.0:29.0, respectively (Table 1).

Analytical methods

PO_4^{3-}-P and NH_4^+-N concentrations were determined according to *Standard Methods* (APHA 2012). Mg^{2+} and Ca^{2+} concentrations were analyzed by ionic chromatography using a Metrohm 861 Advanced Compact IC equipped with a Metrosep A Supp 5-250 column and an 853 CO_2 suppressor. Bicarbonate concentration was related to the concentration of inorganic carbon (IC). IC concentration was determined by a Shimadzu analyzer (TOC-5000) coupled to an automated sampling system (Shimadzu, ASI-5000-S).

Solid samples were taken from the crystallization system for observation and analysis during the experimental time. These samples were fractionated to determine the crystal size distribution. This analysis was carried out using a series of stacked mesh sieves with different size openings. Four fractions of the solid samples were obtained; the range of fractions were: smaller than 0.5 mm (hereafter referred to as fine crystals), between 0.5 and 1.0 mm, between 1.0 and 2.0 mm and larger than 2.0 mm. For a better understanding, pellets have been defined as the precipitates with a size higher than 0.5 mm. Then, the solid samples were dried at 45 °C for 24 h in order to avoid struvite thermal decomposition (Bhuiyan *et al.* 2008). The dried solid samples were weighed and their relative abundance was determined.

The appearance of the precipitates was analyzed by using a scanning electron microscope (SEM, ZEISS EVO®LS 15) coupled to an energy dispersive X-ray microanalysis detector (EDX, Oxford 300; Leica Microsystems, Cambridge, UK). Meanwhile, the crystalline nature and the semi-quantitative composition of precipitates were determined by X-ray diffraction (XRD, Siemens D505).

RESULTS AND DISCUSSION

Crystallization plant operation

During the operation of the struvite crystallization plant a direct relationship between the operating pH and the efficiency of P recovery was observed. At high values of pH, phosphate concentration in the effluent was low, which suggests that the percentage of P recovery increased with increasing pH (Figure 2(a)). The pH was between 8.0 and 8.6.

Figure 2(a) illustrates that an adequate operating pH could be between 8.3 and 8.4. Phosphate concentration in the effluent at these pH values was similar to values obtained at higher operating pH levels, above 8.4. Moreover, when the struvite crystallization system was operated at pH values lower than 8.4, the amount required of $Mg(OH)_2$ was less than for the crystallization plant operation at pH above 8.4.

Phosphorus recovery efficiency was determined in the two components of the crystallization system, the FBR and the settler. In the FBR, the average phosphate concentration in the effluent was 0.70 ± 0.17 mmol $PO_4^{3-}\cdot L^{-1}$ and 0.75 ± 0.31 mmol $PO_4^{3-}\cdot L^{-1}$ for periods I and II, respectively (Figure 2(b)). Even when the phosphate concentration in the influent for period II was higher than for period I, phosphate concentration in the effluent was similar during the whole operational time. The average phosphate concentration in the settler effluent was 0.53 ± 0.16 mmol $PO_4^{3-}\cdot L^{-1}$ and 0.55 ± 0.20 mmol $PO_4^{3-}\cdot L^{-1}$ in periods I and II, respectively (Figure 2(b)). The aforementioned results indicated that the increment in the influent phosphate concentration enhanced the potential of struvite crystallization, incrementing the percentage of P recovery. Literature data show that the phosphate concentration in wastewater affects the struvite crystallization significantly (Dockhorn 2009; Desmidt *et al.* 2013).

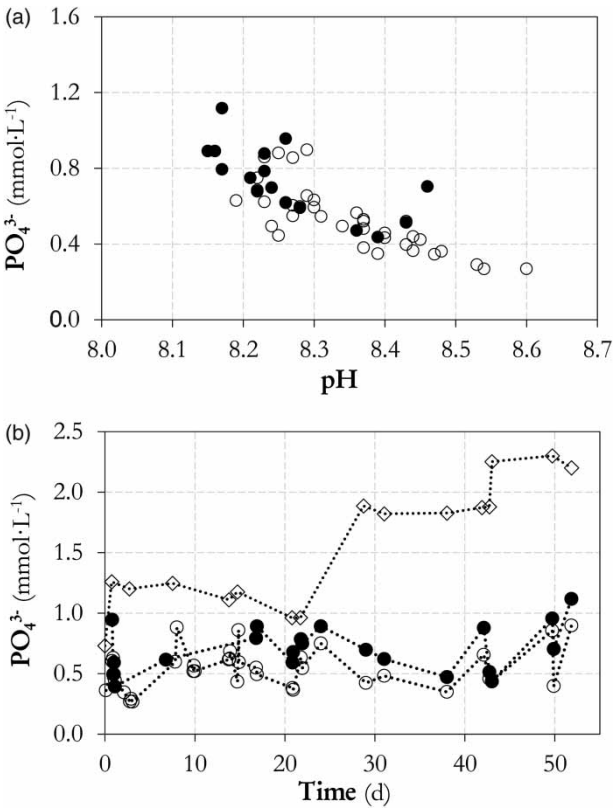

Figure 2 | (a) Phosphate concentration in the effluent of FBR (●) and settler (○) versus operating pH and (b) evolution of phosphate concentration in the influent (◇), FBR effluent and settler effluent during the experimental operation.

The overall percentage of phosphate crystallization was 60.1% for period I, and then it increased up to 76.7% for period II. Most of the phosphate recovery occurred in the FBR. Phosphate recovery percentage in the FBR has been calculated considering the effect of the recirculation flow on the concentration of phosphate in the FBR influent. The recirculation ratio was maintained around 1.0 during the whole operational time. Around 28.4% and 63.6% of the phosphate entering the FBR was converted to struvite in a few minutes during the periods I and II, respectively. The HRT of FBR was between 1.3 and 2.6 minutes. This time represents about 2% of the overall HRT, which was between 75.5 and 137.6 minutes. Thus, a high amount of phosphate that entered the FBR was converted to struvite in less than 3 min. These experimental results corroborate the results presented in Crutchik & Garrido (2016); struvite crystallization is a rapid reversible reaction. According to the struvite crystallization model developed in Crutchik & Garrido (2016), equilibrium conversion can be obtained in a few minutes. Thus, the observed phosphate concentration of the settler effluent was not affected by the phosphate fed, but by the operating conditions.

On the other hand, ammonium concentration in the effluent remained constant during the operation time, with an average concentration of 64.6 ± 5.3 mmol $NH_4^+\cdot L^{-1}$. The decrease of ammonium concentration, around 5 mmol$\cdot L^{-1}$, was higher than the expected values by the crystallization of struvite, which should be less than 1.5 mmol$\cdot L^{-1}$. Free ammonia concentration was around 4.5 mmol$\cdot L^{-1}$, and corresponded to around 7% of total ammonium in the influent. These results indicated that the higher reduction of ammonium was caused by the stripping of free ammonia, which is in agreement with the results reported by other authors (Uludag-Demirer & Othman 2009).

Regarding magnesium ion, magnesium concentration in the influent was relatively stable during the operation of the crystallization system. Magnesium concentration was 0.5 ± 0.1 mmol $Mg^{2+}\cdot L^{-1}$, which was lower than phosphate and ammonium concentrations. So, magnesium was the limiting factor to recover P by struvite crystallization and was supplied by adding an industrial $Mg(OH)_2$ slurry. As mentioned above, $Mg(OH)_2$ slurry was used as magnesium source as well as alkali source. During the operation of the crystallization plant, the dissolved concentration of magnesium in the FBR effluent was around 1.6 ± 0.9 mmol $Mg^{2+}\cdot L^{-1}$, while magnesium concentration in the settler effluent was 1.2 ± 0.6 mmol $Mg^{2+}\cdot L^{-1}$ and 1.5 ± 0.8 mmol $Mg^{2+}\cdot L^{-1}$ for periods I and II, respectively. Magnesium concentration was slightly higher in the FBR effluent than in the settler effluent because magnesium was involved in precipitation reactions, mainly for struvite crystallization and/or magnesium carbonates precipitation. Magnesium concentration in the effluent was mainly associated with the magnesium from the industrial $Mg(OH)_2$ added, which did not react in the crystallization system.

Regarding calcium ions, calcium concentration in the influent remained constant throughout the operation time, with an average concentration of 1.7 ± 0.3 mmol $Ca^{2+}\cdot L^{-1}$ and 1.8 ± 0.2 mmol $Ca^{2+}\cdot L^{-1}$. Meanwhile, calcium concentration in the effluent was 1.1 ± 0.5 mmol $Ca^{2+}\cdot L^{-1}$ and 1.6 ± 0.1 mmol $Ca^{2+}\cdot L^{-1}$ for periods I and II, respectively. The difference between influent and effluent concentrations can be associated with the formation of calcium carbonates. This was because, as mentioned in Crutchik & Garrido (2011), the formation of calcium phosphate was not favored over struvite crystallization because of the high molar ratio of ammonium to phosphate in the influent, which was higher than 32 mol/mol for the whole experimental time.

On the other hand, the treated influent had a high alkalinity with an average IC concentration of 65.2 ± 2.6 mmol $HCO_3^-\cdot L^{-1}$ Bicarbonate concentration in the effluent was around 63.6 ± 3.8 mmol $HCO_3^-\cdot L^{-1}$. The difference between influent and effluent concentrations can be associated with the formation of magnesium and/or calcium carbonates.

Analysis of the solid phase

Precipitates size distribution

Whilst the efficiency of the crystallization process is mainly affected by the wastewater composition and operating conditions, the characteristics of obtained precipitates are very much influenced by the reactor hydrodynamics and the phosphate loading rate. From a hydrodynamic point of view, the hydraulic shear forces affect the size of the precipitates because the shear forces break the precipitates into smaller fractions, fine precipitates. Fine precipitates are more likely to be washed out with the effluent, decreasing the recovery of precipitates. Thus, reactor hydrodynamics may affect the quantity and quality of the produced precipitates. The characteristics of precipitates are directly correlated to the precipitate's recovery efficiency.

Fine precipitates grew during the operation of the crystallization plant, and subsequently these precipitates agglomerated especially in the FBR to form pellets. The pellets grew by assimilating remaining crystals of lower size. This indicates that the heterogeneous crystallization was promoted rather than homogeneous crystallization. In period I, most of the precipitates had a size less than 0.5 mm; in fact, around 76.0% of the solid phase corresponded to fine precipitates, while the remaining 24.0% of the solid phase corresponded to pellets. Therefore, the solid phase obtained in period I was mainly a powder, which had not an adequate particle size for its use as fertilizer because it is more difficult to handle, in terms of storage and transport, than pellets.

The amount of fine precipitates was reduced (40.0%) for period II (Figure S1 in the Supporting Information, available with the online version of this paper). This significant reduction can be associated with the increase of the influent phosphate concentration (Table 1). The increase in phosphate concentration provided a greater potential for struvite crystallization, which directly affected the size and appearance of those precipitates. Ping *et al.* (2016) also found that the purity and size of struvite pellets were more affected for struvite crystallization from wastewater with low P concentrations than from wastewater with high levels of P. In this regard, the fraction of pellets with a size between 0.5 and 1.0 mm was increased from 7.0% (period I) to 24.0% (period II). A similar increase was observed in pellets with a size range between 1.0 and 2.0 mm, which was increased from 12.0% (period I) to 32.0% (period II). Meanwhile, the amount of pellets higher than 2.0 mm was around 5.0% for the whole experimental time. Figure 3 shows the precipitate pellets obtained for period II. The aforementioned results indicate that the hydrodynamics conditions of FBR and the increase of phosphate concentration favored the pellet formation.

The results obtained in this study are in general agreement with previous studies. In the literature, a wide size range of precipitates obtained during the operation of pilot- or full-scale reactors has been reported. The size of produced

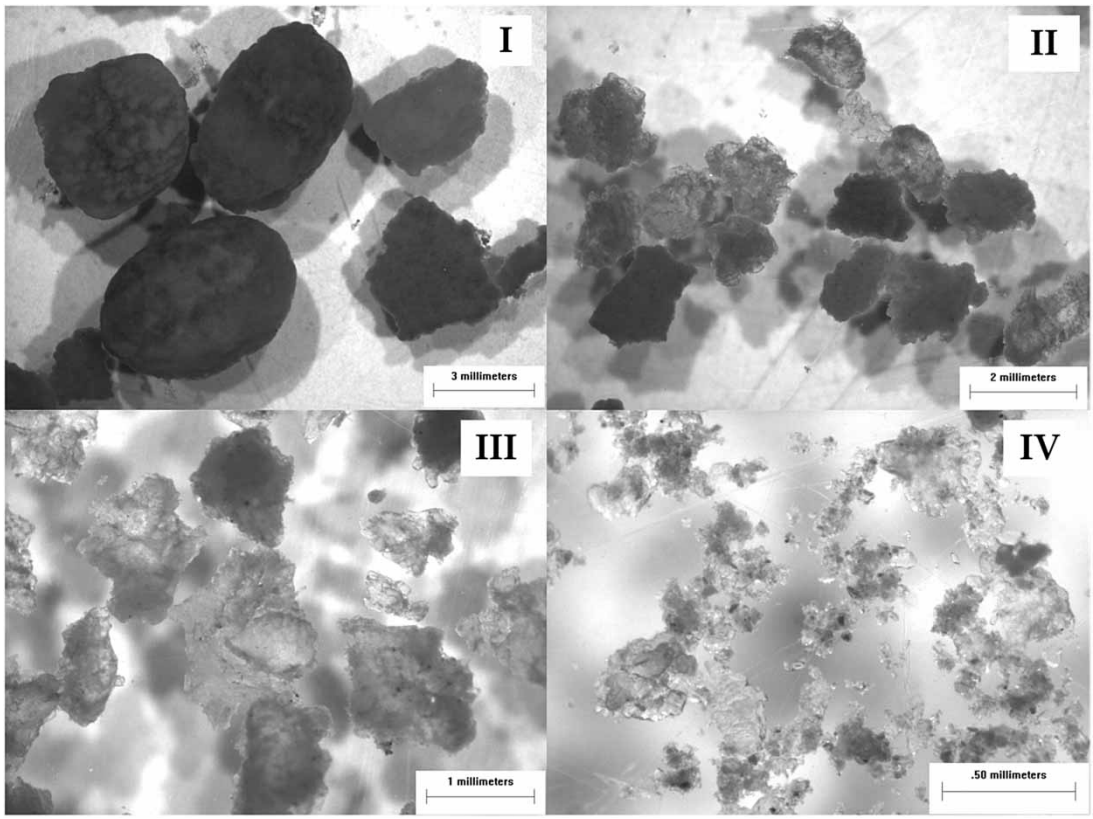

Figure 3 | Image of the precipitate samples of period II used in precipitate size distribution analysis, with the size range: (I) >2.0 mm; (II) 2.0–1.0 mm; (III) 1.0–0.5 mm; (IV) <0.5 mm.

struvite varies from 0.5 mm (Ueno & Fujii 2001) to 6.0 mm (Moerman *et al.* 2009). Moerman *et al.* (2009) obtained struvite pellets with sizes of 2.0–6.0 mm in a full-scale stirred tank crystallizer. Abe (1995) reported struvite pellet sizes of 2.0 ± 3.8 mm in an FBR using sand as seeding material. Ueno & Fujii (2001) obtained struvite crystals with sizes of 0.5–1.0 mm in a full-scale FBR. Remy *et al.* (2013) have obtained an average size of the struvite crystals recovered in a continuously aerated reactor of 0.7 mm. Battistoni *et al.* (2005) have used two different crystallization systems, packed and FBRs, at pilot scale. These authors reported sizes of struvite pellets between 0.5 and 1.4 mm in the packed bed reactor and no higher than 0.5 mm in the FBR. Additionally, Abe (1995) and Moerman *et al.* (2009) stated that the size of produced precipitates is influenced by the P concentration in the influent of the crystallization system.

Appearance and composition of the solid phase

For period I, SEM-EDX microphotographs showed that the solid phase was composed of larger and fine precipitates (Figure S2A in the Supporting Information, available with the online version of this paper). Two types of fine precipitates can be identified: crystals with a needle-like shape and small precipitates. Meanwhile, the larger precipitates were shaped like spherical (pellets), which were formed by the agglomeration of needle-like crystals and small precipitates with an amorphous appearance.

For this period, XRD results detected that phosphorus was crystallized as struvite and trimagnesium phosphate (cattiite, $Mg_3(PO_4)_2{\cdot}22H_2O$). The crystalline nature and the semi-quantitative composition of precipitates are shown in Figure S3 and Table S1 in the Supporting Information (available with the online version of this paper). The struvite co-precipitation with this magnesium phosphate was probably due to the high molar ratio of Mg^{2+}/PO_4^{3-} (Korchef *et al.* 2011). Many authors are in agreement that the presence of an excess of magnesium concentration does not have a positive effect on the struvite crystallization (Korchef *et al.* 2011; Desmidt *et al.* 2013). This is because a high magnesium concentration can promote the magnesium phosphates or/and magnesium carbonates co-precipitation with struvite, depending on the operating pH. The precipitation of these magnesium precipitates affects the purity of the precipitates.

In addition, the formation of magnesium phosphates reduces the phosphate ions available for struvite crystallization. The amount of cattiite was around 13.0% of the total dry mass of the solid phase. In this period, about 64.0% of fine precipitates was struvite. XRD results determined that the struvite content was 27.0% in the pellets with a size higher than 2.0 mm, and the amount of struvite in pellets with a size range between 0.5 and 2.0 mm was 40.0%. So, phosphorus was mainly recovered as fine struvite crystals for period I.

XRD results corroborated that the difference between the concentration of carbonate in the influent and effluent was due to the formation of calcium and magnesium carbonate precipitates. Magnesium carbonate (nesquehonite, $MgCO_3{\cdot}3H_2O$) was detected in precipitates of period I). The amount of nesquehonite was around 50.0% of the total dry mass in pellets higher than 1.0 mm, while 24.0% of the solid sample was nesquehonite in pellets with a size range between 0.5 and 1.0 mm. Unlike in the case of the pellets, nesquehonite was not detected in the fine precipitates. The formation of this mineral was mainly due to the high level of bicarbonate and magnesium ions in the liquid phase. The formation of these magnesium carbonates reduces the amount of magnesium available for struvite crystallization. Struvite co-precipitation with nesquehonite had also been observed by Sakthivel *et al.* (2012) and Hug & Udert (2013).

Additionally, carbonate ions reacted with calcium ions present in the influent wastewater. Two calcium carbonates were detected by XRD analysis, calcite ($CaCO_3$) and monohydrocalcite (hydrocalcite, $CaCO_3{\cdot}H_2O$). In this regard, the amount of calcite was lower than 6.0% in the pellets and fine precipitates obtained for this period. The fraction of monohydrocalcite was 7.0% in pellets higher than 2.0 mm, and the amount of this calcium carbonate was around 9.0% in pellets with a size between 2.0 and 1.0 mm and fine precipitates. A high amount of monohydrocalcite, 27%, was detected in pellets with size range between 1.0 and 0.5 mm.

For period I, the amount of magnesium carbonate and calcium carbonate was around 50.0% of the total dry mass of precipitates, decreasing the purity of the produced precipitates. Thus, the recovery of phosphorus and struvite purity can be compromised by calcium and/or magnesium carbonates co-precipitation (Le Corre *et al.* 2005; Hao *et al.* 2008; Moerman *et al.* 2009).

Moreover, XRD analysis detected the presence of a small fraction of brucite ($Mg(OH)_2$) in the pellets and fine precipitates. According to semi-quantitative analysis of XRD, the amount of brucite was around 4.0% of the total dry mass. The presence of $Mg(OH)_2$ was attributed to the slurry of $Mg(OH)_2$, which corresponded to the fraction of the $Mg(OH)_2$ added that did not either solubilize or react in the crystallization system.

For period II, in which the influent had a higher phosphate concentration, the nature of precipitates changed (Figure S3 in the Supporting Information). However, SEM-EDX microphotographs showed that the appearance of precipitates was similar in both periods (Figure S2 in the Supporting Information). Regarding the composition of the solid phase, XRD results identified that the most abundant mineral present in the solid phase was struvite. The struvite content was increased from 27.0% to 64.0% in the largest crystals. However, a high level of struvite was detected in the other fractions of the solid phase: it was around 78% in the fine precipitates. Therefore, struvite crystallization was promoted with the increase of phosphate concentration in the influent.

Unlike for period I, nesquehonite was only identified in the largest pellets in period II; the nesquehonite content was 7.0% of the total dry mass. Probably, this quantity of nesquehonite might have been present because of the high level of nesquehonite obtained in period I. This can be explained by the fact that nesquehonite was not detected in the pellets with size less than 2.0 mm or in fine precipitates. According to this, it seems that nesquehonite was not formed in this period. Moreover, the content of calcite in the solid phase was quite similar to that determined in period I; it was around 3%, whilst the amount of monohydrocalcite determined in the solid fractions was slightly lower than in the solid phase of the previous period.

Brucite was not detected in any of the solid fractions during period II. This could indicate that the struvite crystallization plant was able to operate efficiently in terms of $Mg(OH)_2$ added/$Mg(OH)_2$ consumed. Also, the semi-quantitative analysis of XRD determined that the content of cattiite was relatively similar, around 13.0% of the total dry mass, during both experimental periods (Table S1 in the Supporting Information).

Technical and economic evaluation of the use of the industrial $Mg(OH)_2$ slurry for struvite crystallization at full scale

The use of the industrial $Mg(OH)_2$ slurry was evaluated to determine the feasibility of this magnesium product as a magnesium and alkali source for struvite crystallization at full scale. The industrial $Mg(OH)_2$ was a slurry of powdered product in water. Due to the powdered nature of this

product, MgO was not fully converted to $Mg(OH)_2$ as also stated by Matabola *et al.* (2010). However, high chemical conversions of MgO to $Mg(OH)_2$, around 60%, were obtained during the hydration process. During the operation of the struvite crystallization plant, samples of $Mg(OH)_2$ slurry were taken to verify its stability. The obtained results indicated that the characteristics of $Mg(OH)_2$ slurry remained stable during the operation of the crystallization plant (Table S2 in the Supporting Information, available with the online version of this paper). Contrary to the industrial grade MgO, which forms stones of unreacted MgO, $Mg(OH)_2$ does not agglomerate in contact with water at environment temperature. Thus, $Mg(OH)_2$ and not MgO, was chosen as the low cost magnesium and alkali source.

Regarding the efficiency of $Mg(OH)_2$ slurry, the molar ratio of Mg added·P precipitated^{-1} was 7.1 mol Mg added·mol P precipitated^{-1} (16.6 t-industrial Mg product added·t-P recovered^{-1}) for period I. However, the molar ratio of Mg added·P precipitated^{-1} was significantly reduced to 1.5 mol Mg added·mol P precipitated^{-1} (3.5 t-industrial Mg product added·t-P recovered^{-1}) for period II. This reduction in the consumption of $Mg(OH)_2$ slurry was due to the increase of influent phosphate concentration. In this regard, the low phosphate recovery observed for period I can be attributed to the relatively low phosphate concentration in the influent, resulting in low potential for struvite crystallization. Large amounts of chemical (external sources of magnesium and alkali) are necessary in order to obtain an efficient struvite crystallization process. It is important to note that even when the amount of $Mg(OH)_2$ slurry added for period I was around five times higher than for period II, the phosphate concentration in the effluent was more or less constant during the whole experimental period (Figure 2(b)).

The high consumption of $Mg(OH)_2$ slurry observed in period I was also affected by the high alkalinity level. In this study, the main species that contributed to wastewater alkalinity were ammonium and bicarbonate ions. These ions are involved in other equilibrium reactions that release protons, when pH is raised, and consequently it was necessary to add more $Mg(OH)_2$ slurry to achieve the optimal pH range for struvite crystallization. Stratful *et al.* (2001) suggested that an excess of ammonium concentration could be beneficial for struvite crystallization to ensure high struvite crystallization efficiency. Nevertheless, high ammonium concentration increased the requirements for $Mg(OH)_2$ at laboratory scale.

In this work, a chemical equilibrium software, Visual Minteq, (Gustafsson 2010) was used to demonstrate the effect of these ions on the consumption of $Mg(OH)_2$. For simulations, the possible solid phases that might precipitate were specified during the simulations. The mineral species considered were only those that precipitated experimentally during this work (struvite, monohydroclacite, calcite, nesquehonite, and cattiite). For period I, the theoretical $Mg(OH)_2$ consumption to increase the pH from 8.2 to 8.4 was 6.1 t-industrial Mg product added per t-P recovered, which was lower than the experimental value (16.6 t-industrial Mg product added·t-P recovered^{-1}). In contrast, for period II, the predicted $Mg(OH)_2$ consumption was similar to the experimental value to increase the pH from 8.1 to 8.3 (3.4 t-industrial Mg product added·t-P recovered^{-1}). Predicted results corroborate that the consumption of $Mg(OH)_2$ is also affected by ammonium and bicarbonate concentrations (Figure S4 in the Supporting Information, available with the online version of this paper).

The obtained results indicate that phosphate concentration had a higher impact on $Mg(OH)_2$ requirements than the alkalinity level. High efficiencies of struvite crystallization and $Mg(OH)_2$ consumptions were obtained, even when the treated wastewater had a high level of alkalinity. Additionally, an overdose of magnesium ion did not increase the P recovery percentage.

Similar results were obtained by Sánchez *et al.* (2011). Sánchez *et al.* (2011) used an industrial grade magnesium product with a purity in terms of MgO, 68.0%, less than that used in this study (80.5%). Sánchez *et al.* (2011) reported a consumption of an industrial magnesium product for struvite crystallization of 1.6 mol Mg added·mol P precipitated^{-1} in an FBR, which is similar to the consumption obtained in this work (1.5 mol Mg·mol P precipitated^{-1}).

Furthermore, an economic evaluation of the use of the industrial $Mg(OH)_2$ slurry was developed. The operating costs associated with the requirements for $Mg(OH)_2$ slurry were determined considering an estimated cost of industrial magnesium product used (€350·t-$Mg(OH)_2^{-1}$). The estimated costs were around €4,700·t-P precipitated^{-1} and €980·t-P precipitated^{-1} for periods I and II, respectively. The consumed amount of the magnesium product affected directly the economy of the crystallization process.

As previously stated by other authors, high phosphate concentrations make it possible to guarantee the economic viability of the process (Dockhorn 2009; Desmidt *et al.* 2013). In this study, the costs associated with phosphorus concentrations of 2.2 mM (68 mg PO_4^{3-}-P·L^{-1}) were much lower than those estimated using other processes to remove/recover phosphorus from wastewater. In this regard, the cost of phosphorus precipitation by conventional processes, adding aluminum or iron salts, is between €2,000 and €3,000·t-P

precipitated^{-1} (Dockhorn 2009). In struvite crystallization, the cost of the addition of an external magnesium source has been estimated as between €700 and €4,000·t-P precipitated^{-1} (Carballa *et al.* 2009; Dockhorn 2009; Etter *et al.* 2011; Señoráns *et al.* 2011; Sakthivel *et al.* 2012; Hug & Udert 2013). In this regard, a study by Dockhorn (2009) estimated that a general struvite market value is around €700·t-P precipitated^{-1}. The struvite crystallization cost by adding $MgCl_2$ and NaOH is around of €4,000·t-P precipitated^{-1} (Carballa *et al.* 2009); whilst the cost for struvite crystallization by using $MgSO_4$ is estimated at around €2,000·t-P precipitated^{-1} (Etter *et al.* 2011; Sakthivel *et al.* 2012). Similar struvite operating cost has been determined by using magnesium dosing by electro-dissolution (Hug & Udert 2013). On the other hand, Señoráns *et al.* (2011) reported that the operating cost of struvite crystallization at industrial scale was around to €2,900·t-P precipitated^{-1}. These authors have used seawater as magnesium source; in fact, the chemical cost was mainly due to the alkali requirements. These results are in agreement with our findings. Furthermore, it is important to take into account that struvite could be commercialized as agricultural fertilizer. In the literature, the estimated market price of struvite is between €2,000 and €4,500·t-P^{-1} (Münch & Barr 2001; Etter *et al.* 2011; Geerts *et al.* 2015). Therefore, on the basis of our experimental results and literature data for the estimated prices of struvite, the use of this industrial grade magnesium product for struvite crystallization could be economically viable at industrial scale.

CONCLUSIONS

The viability of phosphorus recovery from wastewater in a full-scale crystallization plant has been verified, obtaining struvite pellets with a size range of 0.5–5.0 mm. This produced struvite was suitable to be used as an agricultural fertilizer.

Influent phosphate concentration has an important effect on the crystallization efficiency and the purity of obtained precipitates. Struvite crystallization from wastewater with low phosphate concentration, P concentration lower than 60 mg PO_4^{3-}-P·L^{-1}, is not economically viable because it requires large amounts of chemicals. Also, an inverse relationship between the phosphate concentration in the effluent and the operating pH was observed, in which the optimal operating pH was between 8.3 and 8.4. A high efficiency of phosphorus recovery was obtained, even when the effluent treated had a high level of alkalinity.

The industrial magnesium product can be an economical alternative as magnesium and alkalinity sources for struvite crystallization at full-scale plant, with a $Mg(OH)_2$ requirement of 1.5 mol $Mg(OH)_2$·mol P precipitated^{-1}.

ACKNOWLEDGEMENTS

The authors acknowledge the project Pioneer_STP (ID 199) funded by the WaterWorks2014 Cofunded Call (Water JPI/Horizon 2020). The authors from the University of Santiago de Compostela belong to the Galician Competitive Research Group (GRC 2013-032) programme co-funded by FEDER. The authors gratefully acknowledge the staff of Guillarei WWTP and 'Consorcio de Augas do Louro' for their assistance, the process control and optimization group of the Chemical Engineering Department, UVigo, for the assistance with automation of the plant, and the members of Magnesitas de Rubian that kindly provided the industrial grade magnesium oxide product.

REFERENCES

Abe, S. 1995 Phosphate removal from dewatering filtrate by MAP process at Seibu treatment plant in Fukuoka City. *Sewage Works in Japan*, pp. 59–64.

APHA 2012 *Standard Methods for the Examination of Water and Wastewater*, 22nd edn. American Public Health Association/American Water Works Association/Water Environment Federation, Washington, DC, USA.

Battistoni, P., Paci, B., Fatone, F. & Pavan, P. 2005 Phosphorus removal from supernatants at low concentration using packed and fluidized-bed reactors. *Industrial & Engineering Chemical Research* **44**, 6701–6707.

Bhuiyan, M. I., Mavinic, D. S. & Koch, F. A. 2008 Phosphorus recovery from wastewater through struvite formation in fluidized bed reactors: a sustainable approach. *Water Science and Technology* **57**, 175–181.

Carballa, M., Moerman, W., De Windt, W., Grootaerd, H. & Verstraete, W. 2009 Strategies to optimize phosphate removal from industrial anaerobic effluents by magnesium ammonium phosphate (MAP) production. *Journal of Chemical Technology and Biotechnology* **84**, 63–68.

Crutchik, D. & Garrido, J. M. 2011 Struvite crystallization versus amorphous magnesium and calcium phosphate precipitation during the treatment of a saline industrial wastewater. *Water Science and Technology* **64**, 2460–2467.

Crutchik, D. & Garrido, J. M. 2016 Kinetics of the reversible reaction of struvite crystallisation. *Chemosphere* **154**, 567–672.

Desmidt, E., Ghyselbrecht, K., Monballiu, A., Rabaey, K., Verstraete, W. & Meesschaert, B. D. 2013 Factors influencing urease driven struvite precipitation. *Separation and Purification Technology* **110**, 150–157.

Dockhorn, T. 2009 About the economy of phosphorus recovery. In: *International Conference on Nutrient Recovery from Wastewater Streams*, IWA Publishing, London.

Etter, B., Tilley, E., Khadka, R. & Udert, K. M. 2011 Low-cost struvite production using source-separated urine in Nepal. *Water Research* **45**, 852–862.

Forrest, A. L., Fattah, K. P., Mavinic, D. S. & Koch, F. A. 2008 Optimizing struvite production for phosphate recovery in WWTP. *Journal of Environmental Engineering* **134**, 395–402.

Geerts, S., Marchi, A. & Weemaes, M. 2015 Full-scale phosphorus recovery from digested wastewater sludge in Belgium – Part II: economic opportunities and risks. *Water Science and Technology* **71**, 495–502.

Gustafsson, J. P. 2010 *Visual Minteq Version 3.0 Beta*. KTH, Department of Land and Water Resources Engineering, Stockholm, Sweden.

Hao, X. D., Wang, C. C., Lan, L. & van Loosdrecht, M. C. 2008 Struvite formation analytical methods and effects of pH and Ca^{2+}. *Water Science and Technology* **58**, 1077–1083.

Hug, A. & Udert, K. M. 2013 Struvite precipitation from urine with electrochemical magnesium dosage. *Water Research* **47**, 289–299.

Koch, F. A., Mavinic, S., Yonemitsu, N. & Britton, A. T. 2009 Fluidized bed wastewater treatment. United States patent no. US 7622047 B2.

Korchef, A., Saidou, H. & Ben Amor, M. 2011 Phosphate recovery through struvite precipitation by CO_2 removal: effect of magnesium, phosphate and ammonium concentrations. *Journal of Hazardous Materials* **186**, 602–613.

Le Corre, K. S., Valsami-Jones, E., Hobbs, P. & Parsons, S. A. 2005 Impact of calcium on struvite crystal size, shape and purity. *Journal of Crystal Growth* **283**, 514–522.

Matabola, K. P., van der Merwe, E. M., Strydom, C. A. & Labuschagne, F. J. W. 2010 The influence of hydrating agents on the hydration of industrial magnesium oxide. *Journal of Chemical Technology and Biotechnology* **85**, 1569–1574.

Moerman, W., Carballa, M., Vandekerckhove, A., Derycke, D. & Verstraete, W. 2009 Phosphate removal in agro-industry: pilot- and full-scale operational considerations of struvite crystallization. *Water Research* **43**, 1887–1892.

Münch, E. & Barr, K. 2001 Controlled struvite crystallisation for removing phosphorus from anaerobic digester sidestreams. *Water Research* **35** (1), 151–159.

Ping, Q., Li, Y., Wu, X., Yang, L. & Wang, L. 2016 Characterization of morphology and component of struvite pellets crystallized from sludge dewatering liquor: effects of total suspended solid and phosphate concentrations. *Journal of Hazardous Materials* **310**, 261–269.

Rahman, Md. M., Salleh, M. A. M., Rashid, U., Ahsan, A., Hossain, M. M. & Ra, C. S. 2014 Production of slow release crystal fertilizer from wastewaters through struvite crystallization – a review. *Arabian Journal of Chemistry* **7**, 139–155.

Remy, M., Driessen, W., Hendrickx, T. & Haarhuis, R. 2013 Recovery of phosphorus by formation of struvite with the Phosphaq™ process. In: *18th European Biosolids and Organic Resources Conference*.

Sakthivel, S. R., Tilley, E. & Udert, K. M. 2012 Wood ash as a magnesium source for phosphorus recovery from source-separated urine. *Science of the Total Environment* **419**, 68–75.

Sánchez, E., Rodríguez, B., Heredero, R., García Peñuela, R., Polo, A., García, M., Plaza, C., García, E. & Sanz, R. 2011 Experiencias para la recuperación del fósforo de las aguas residuales en forma de estruvita en Canal de Isabel II. Cuadernos de I + D + I.

Señoráns, L., Barros, S., García, G. & Garrido, J. M. 2011 Phosphorus recovery by struvite crystallization in a wastewater from a frozen fish factory. *Tecnología del Agua* **335**, 26–35 (in Spanish).

Stratful, I., Scrimshaw, M. D. & Lester, J. N. 2001 Conditions influencing the precipitation of magnesium ammonium phosphate. *Water Research* **35**, 4191–4199.

Ueno, Y. & Fujii, M. 2001 Three years experience of operating and selling recovered struvite from full-scale plant. *Environmental Technology* **22**, 1373–1381.

Uludag-Demirer, S. & Othman, M. 2009 Removal of ammonium and phosphate from supernatant of anaerobically digested waste activated sludge by chemical precipitation. *Bioresource Technology* **100**, 3236–3244.

First received 10 August 2016; accepted in revised form 2 November 2016. Available online 16 November 2016